Conformational Stability of a Model Macrocycle Tetraamide: An ab Initio Study

Rubén D. Parra,* Brian Yoo, and Mike Wemhoff

Department of Chemistry, DePaul University, Chicago, Illinois 60614

Received: January 6, 2006; In Final Form: February 10, 2006

Ab initio calculations are carried out to investigate the conformational stability of a model macrocyle tetraamide. The four amide groups in the selected model are present in the sequence: −(O═CNH)−Ph−(NHC═O)−CH═CH−(O═CNH)−Ph−(NHC═O)−CH═CH−. In this sequence, two phenyl rings and two ethene groups act as bridges between the amide units. Each amide motif bonds to a phenyl ring through its amide nitrogen and to an ethene group through its amide carbon. Four clearly distinct minimum-energy conformations are found upon full geometry optimization using the B3LYP/6-31+G(d) method. Frequency calculations using the same method confirm that the four conformations are indeed minima in the macrocycle potential energy surface. Relative to the most stable conformer, the other conformations are higher in energy by 0.86, 2.09, and 9.17 kcal/mol, respectively, at the MP2/6-31+G(d,p) level. The stability of the macrocycle conformations is correlated primarily to the existence and strength of intramolecular N−H···O═C hydrogen bonds. Additional stability to the conformations is found to come from weak Ph−H···O═C hydrogen bonding between a carbonyl oxygen and a hydrogen atom of a phenyl group. Solvent effects play an important role in the relative energies of the various conformations, as indicated by the simple SCRF = dipole model calculations for the case of aqueous solution.

Introduction

Macrocyclic molecules form stable complexes with ions by providing many binding sites directed toward the guest ion in a convergent manner. Accordingly, macrocyclic molecules can be designed to have a definite cavity size so that ions whose size fits better into the cavity will be selectively bound.[1] The remarkable selectivity of ions by macrocycles illustrates the principle of molecular recognition and is the basis of many applications.[2] Perhaps the most widely known and extensively investigated macrocycles are the so-called crown ethers which exhibit strong affinity and high selectivity for alkali and alkaline earth metal ions.[3] Some other widely investigated macrocyclic hosts include cryptands,[4] starands,[5,6] cyclodextrines,[7] and calixarenes.[8]

Macrocyclic amides form another group of ion receptors that have been given considerable attention. A number of recent publications have presented convincing evidence that, depending on the experimental conditions, macrocyclic amides can bind cations or anions.[9] In general, the complexation process will be energetically more favorable if the preferred conformation of the macrocycle in the free state resembles closely the conformation it will adopt upon interaction with the host ion or ions. Thus, an important research endeavor is the study of the conformational stability of potential ion receptors in the absence of any host ions. The purpose of this research is to carry out a computational ab initio study of the conformational stability of a model macrocyclic tetraamide. The relative stabilities of the different conformers is rationalized in terms of the intramolecular interactions of the amide groups in the particular macrocycle conformation. The effects of the surrounding environment on the stability of the conformations is examined using the Onsager reaction field model which represents solvents of differing polarity by means of their characteristic dielectric constants.

* To whom correspondence should be addressed. E-mail: rparra1@depaul.edu.

Method of Calculations

Ab initio calculations were carried out with the GAUSSIAN 03 program.[10] Geometry optimizations were first performed at the B3LYP[11,12] level using the 6-31G(d) basis set[13] and then the so-optimized geometries were further optimized using the 6-31+G(d) basis set.[14] This higher method was used to obtain the vibrational frequencies and verify that the optimized structures were indeed minima in the potential energy surface. Single-point energy calculations were performed using 6-31+G(d) and 6-31+G(d,p)[13−15] basis sets at the MP2 level.[16] The optimized geometries were subjected to natural bond orbital (NBO) analysis performed on wave functions calculated at the HF/6-31+G(d,p) level.[17] The theory of atoms in molecules (AIM) approach was used to calculate critical-point electron densities along the intramolecular hydrogen bonds.[18] The gauge-including atomic orbital (GIAO) approach was used to compute ^{1}H NMR chemical shifts, relative to the standard TMS, at the B3LYP/6-311+G(2d,p) level.[19] The SCRF = dipole Onsager model was employed to explore solvent effects on the stability of the various macrocycle conformations.[20] The HF and MP2 methods with the 6-31+G(d) basis set were used for the calculations using the dielectric constant of water, $\epsilon = 78.39$.

Results and Discussion

Macrocyclic Tetraamide Conformations. The model macrocycle tetraamide considered here can be thought of as being built from two parent diamide motifs and two additional RCH═CHR molecules containing the ethene bridging units. The parent diamide motifs are displayed in Figure 1 and are conveniently labeled A, B, and C. Also shown in Figure 1 is the atomic numbering scheme used for discussion.

10.1021/jp060120e CCC: $33.50
Published on Web 03/14/2006

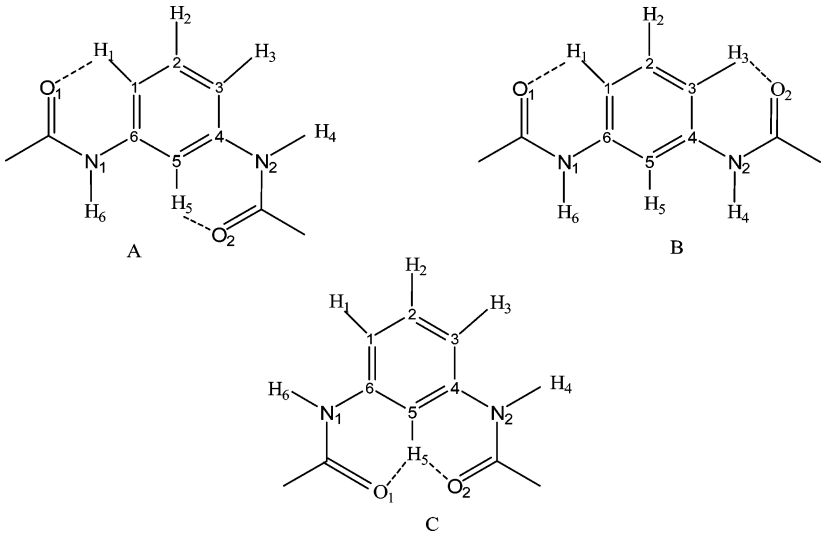

Figure 1. Parent diamide motifs A, B, and C used to build up the model macrocycle tetraamide studied in this work.

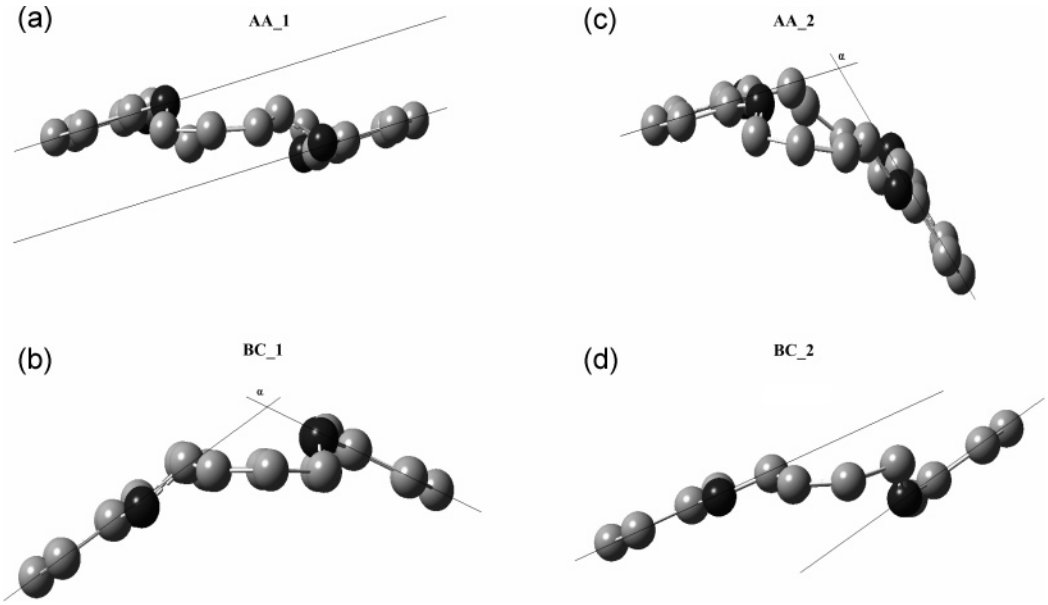

Figure 2. Side view of the B3LYP/6-31+G(d) optimized macrocycle conformations AA_1, AA_2, BC_1, and BC_2. Hydrogen and oxygen atoms omitted for clarity.

Four distinct minimum-energy structures were identified for the macrocyclic tetraamide at the B3LYP/6-31+G(d) level. The opt = tight convergence option was used, and no symmetry constraints were imposed during the geometry optimizations. Frequency calculations carried out at the same level of theory confirmed that all structures are indeed minima on the potential energy surface. The four conformations of the tetraamide are shown in Figures 2 and 3, and are labeled AA_1, AA_2, BC_1, and BC_2, respectively. The labels are chosen to reflect the combination of the parent diamide motifs giving rise to the particular conformation. Thus, suitable combinations of the parent motif A result in the two different macrocycle conformations AA_1 and AA_2; similarly, combinations of the parent motifs B and C result in the other two macrocycle conformations. No suitable combinations of type BB or CC were found to result in minimum-energy structures of the macrocycle. Although no symmetry constraints were imposed, the optimized conformations belong to the point groups C_i (AA_1), C_2 (AA_2), and C_s (BC_1 and BC_2). In the building of the macrocyle, two bridging units containing the ethene C═C motif are required in addition to the parent diamides.

A first general impression of the similarities and differences of the four minima can be gleaned from the side view displays shown in Figure 2, which shows the orientation of the carbon and nitrogen atoms, that is, the backbone of the macrocycle. Except for AA_2, the four carbon atoms of the two ethene groups lie in the same plane. The planes of the benzene rings are found to be inclined relative to the plane formed by the ethene carbon atoms. However, the relative orientation of the benzene rings differs in the three structures AA_1, BC_1, and BC_2. Briefly, AA_1 is seen to adopt a stairlike conformation with the two benzene rings almost parallel to each other. The center of inversion of the molecule is actually located in the plane formed by the two ethene groups. BC_2 adopts a more chairlike orientation with one of the benzene rings tilted with respect to the other benzene ring. The corresponding imaginary lines that pass through the opposing hydrogen atoms in each benzene ring intersect at a point far (~20 Å) from the plane of the ethene groups and are at an angle of about 8°. BC_1 orientation resembles that of a boatlike conformation; the corresponding imaginary lines that pass through the opposing hydrogen atoms in each benzene ring intersect at a point close

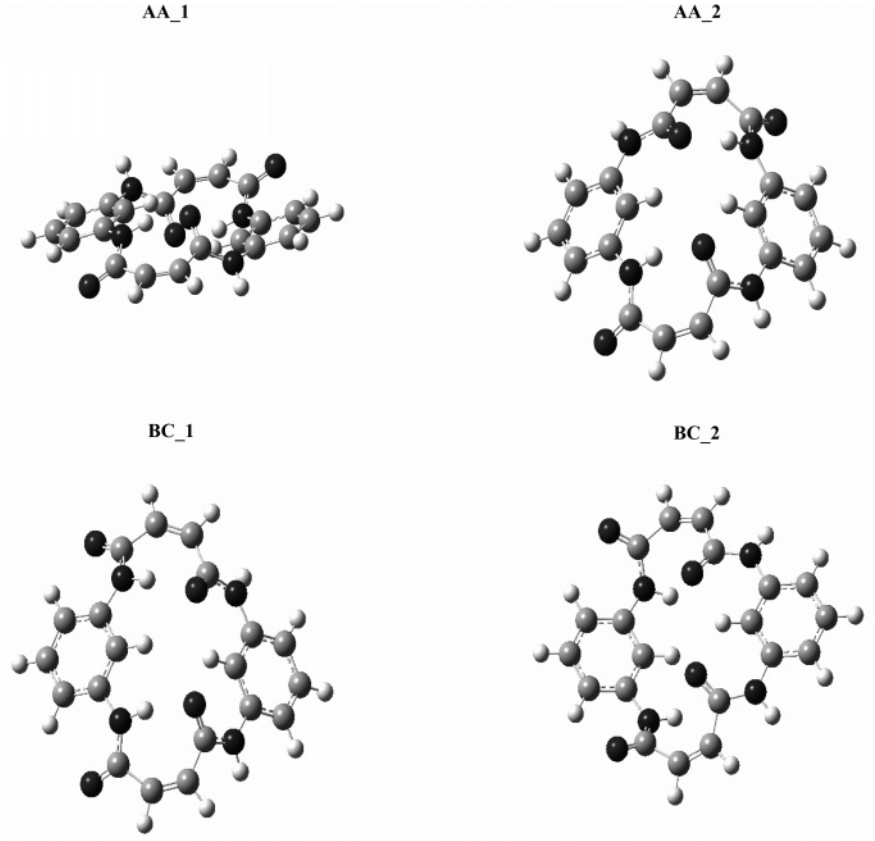

Figure 3. Top view of the B3LYP/6-31+G(d) optimized macrocycle conformations AA_1, AA_2, BC_1, and BC_2.

to and above the plane formed by the ethene groups and are at an angle, which is labeled α in Figure 2, of about 127°. In contrast, the four carbon atoms of the ethenyl groups in AA_2 are twisted by about 24°. Thus, AA_2 resembles the twist-boat conformation of cyclohexane. The corresponding value of α for AA_2 is 118°.

The relative orientation of the amide C═O and N−H groups in the different conformations are appreciated in Figure 3 which shows that two of the four carbonyl oxygen atoms are directed inward (toward the central cavity of the molecule) and the others are directed outward. Except for BC_2, there are two equivalent N−H···O═C hydrogen bonds between corresponding amide units which are pointing inward. The strength of the intramolecular H-bonds plays a major role in the relative stability of the various conformations of the tetraamide macrocycle as discussed later.

Geometry Parameters. In an effort to present a unified discussion of the structural parameters, we chose to focus on bond distances, angles, and dihedrals involving directly the amide motif H−N−C═O, and the results are displayed in Table 1. A distinctive feature in A, B, and C is the presence of two unconventional H-bond interactions each between a carbonyl oxygen and a hydrogen from the aromatic ring (see Figure 1). Upon formation of the macrocycle, one of these H-bonds (C_1H_1···O_1) will be located away from the central cavity, whereas the other (C_5H_5···O_2) will be a component of the central cavity. For convenience, the former H-bond will be referred to as the outward H-bond and the latter as the inward H-bond. From the H-bond distances shown in Table 1, it appears that the inward C−H···O hydrogen bond is stronger than the outward one. For example, although each of the C−H···O H-bonds forms a six-membered ring in structure A, the H_5···O_2 distance is 0.037 Å shorter than that in H_1···O_1. Also, having two outward H-bonds (structure B) appears to have a rather small effect on the strength of the individual outward H-bond, that is, the H···O is lengthened by only 0.006 Å relative to that in structure A. In contrast, having two inward H-bonds (structure C) weakens the individual C−H···O interactions as manifested in the noticeable elongation (0.050 Å) of the H-bond distance relative to structure A. These conclusions are further confirmed upon inspection of the electron densities calculated at the critical points along these H-bonds and whose values are exhibited in Table 2. Thus, the electron density for the inward H-bond in C is about 11% smaller than that in A indicating negative cooperativity upon formation of the three-center H-bond in C. The reduction of electron density in the outward H-bond is just about 1% in B relative to that in A.

Formation of the macrocycle results in a sizable reduction of the strength of the outward C−H···O hydrogen bond relative to that in the corresponding parent diamide motif. This is apparent in the lengthening of the H_1···O_1 distance and the loss of planarity of the six-membered ring of the H-bond as indicated by the O_1···$H_1C_1C_6$ dihedral. The effect is most dramatic in BC_2 where the H_1···O_1 distance is the longest (2.468 Å) and the magnitude of the dihedral O_1···$H_1C_1C_6$ is the greatest (∼26°). Again, the electron densities at the critical points shown in Table 2 confirm the geometrical results. It is seen, for example, that all macrocycle conformations result in a decrease of the electron density along the outward C−H···O hydrogen bond, with BC_2 having the most change and AA_2 having the least. As for the inward C−H···O hydrogen bond, AA_1 results in a complete loss of this interaction with a H_5···O_2 distance of 2.597 Å and a dihedral O_2···$H_5C_5C_4$ of −44.7°. The other three conformations, however, exhibit a somewhat stronger inward C−H···O interaction in each case with an H_5···O_2 distance appreciably shorter than that in the corresponding parent motif. Although the planarity of the six-membered ring is lost,

TABLE 1: B3LYP/6-31+G(d) Relevant Bond Distances (Å), Angles, and Dihedrals (deg) for Parent Diamides and Macrocycle Conformations

system	$H_1\cdots O_1$	$H_5\cdots O_2$	N−H···O	$C_1H_1\cdots O_1$	$C_5H_5\cdots O_2$	N−H···O
A	2.263	2.226		119.5	121.0	
B	2.269			119.5		
C		2.276			119.2	
AA_1	2.411	2.597	1.728	112.8	95.8	160.1
AA_2	2.372	2.139	1.790	113.7	120.3	155.3
BC_1	2.413	2.215	1.832	113.1	117.1	150.5
BC_2	2.468	2.122	2.496	110.6	120.6	98.7

system	$C{=}O_1$	$C{=}O_2$	N_1-H_6	N_2-H_4	$C-N_1$	C_6-N_1	$C-N_2$	C_4-N_2
A	1.220	1.221	1.013	1.013	1.371	1.413	1.370	1.414
B	1.219	1.219	1.013	1.013	1.372	1.414	1.372	1.414
C	1.217	1.217	1.013	1.013	1.374	1.413	1.374	1.413
AA_1	1.231	1.237	1.025	1.013	1.365	1.409	1.369	1.433
AA_2	1.231	1.236	1.022	1.013	1.367	1.411	1.369	1.423
BC_1	1.231	1.233	1.020	1.013	1.364	1.415	1.374	1.420
BC_2	1.225	1.226	1.011	1.012	1.373	1.419	1.385	1.416

system	$O_1\cdots H_1C_1C_6$	$O_2\cdots H_5C_5C_4$	$H_6-N_1\cdots C_6C_5$	$H_4-N_2\cdots C_4C_3$
A	0.0	0.0	0.0	0.0
B	0.0	0.0	0.0	0.0
C	0.0	0.0	0.0	0.0
AA_1	−21.4	−44.7	10.9	53.5
AA_2	−20.2	3.1	8.4	−11.9
BC_1	−20.9	−11.1	6.2	176.9
BC_2	−25.8	−14.0	6.5	175.5

TABLE 2: HF/6-31+G(d,p) Critical-point Densities (au) along the Hydrogen Bonds[a]

		inward[b]	outward[b]
system	N−H···O=C	C=O···H	C=O···H
A		0.0175	0.0164
B			0.0162
C		0.0155	
AA_1	0.0430		0.0127
AA_2	0.0375	0.0208	0.0136
BC_1	0.0346	0.0179	0.0127
BC_2		0.0211	0.0116

[a] For every H-bond listed here there is another one symmetrically equivalent. The exception is system A for which the two possible H-bonds are listed. [b] A C=O···H interaction is labeled inward or outward based on whether such interaction points, respectively, toward or away from the central cavity upon formation of the macrocycle.

the magnitude of the dihedral change is much smaller than that observed in AA_1.

The changes in electron densities at the corresponding H-bond critical points mirror the geometrical results. In fact, by considering only the distortions on the existing C−H···O hydrogen bonds in the parent motifs, reflected, for example, in the critical-point densities (Table 2), we see that AA_1 and BC_1 present a loss of electron density, while AA_2 and BC_2 present an overall favorable increase. In the particular case of AA_1, the critical-point electron density along the C−H···O hydrogen bond is only 0.0127 compared with 0.0339 in A. In contrast, the combined (inward + outward) electron density along the C−H···O critical points in AA_2 is 0.0344. Thus, in AA_2, the strengthening of the inward C−H···O bond more than compensates for the weakening of the outward C−H···O bond upon macrocycle formation. Likewise, while the combined electron density along the C−H···O critical points in BC_1 is a bit lower than 0.0317, which is the result obtained by adding the critical densities of the outward C−H···O in B and the inward C−H···O in C, the combined electron density in BC_2 is actually greater. It should be noted that, with the exception of BC_2, macrocycle formation results in two new conventional N−H···O hydrogen bonds which help stabilize the different conformations as discussed next.

Energetics. MP2 single-point energy calculations were performed on the B3LYP/6-31+G(d) optimized geometries of the diamide motifs and the various conformations of the macrocycle tetraamide. The 6-31+G(d), 6-31+G(d,p), and 6-311++G(2d,2p) basis sets were employed for diamides, whereas only the first two of these basis sets were employed for the macrocycle conformations. Zero-point energy corrections were obtained using the harmonic frequencies obtained with the same level of theory used for geometry optimizations, that is, B3LYP/6-31+G(d).

The different levels of calculations agree on the relative stability of the parent diamides A > B > C. Correlation corrections through MP2 or the density functional B3LYP reduce the energy separation among the parent motifs. Thus, while C is 3.04 kcal/mol higher in energy than A at the HF/6-31+G(d) level, this difference is reduced to 2.78 and 2.55 kcal/mol using the same basis set and the B3LYP and MP2 methods, respectively. Increasing the size of the basis set generally reduces the energy separation of B and C relative to A. Conformation C with a three-center H-bond interaction appears to be the one that benefits the most by improving both the correlation correction and the size of the basis sets. The relative stability of the various conformations of the macrocycle tetraamide, AA_1 > AA_2 > BC_1 ≫ BC_2, is found to be consistent both at the HF and at the MP2 levels and at the two basis sets used, 6-31+G(d) and 6-31+G(d,p). The B3LYP level, however, finds AA_2 more stable than AA_1. Correction for zero-point energies using the calculated harmonic vibrational frequencies results in AA_2 being more stable than AA_1 at the HF level.

The relative stability of the various macrocycle's conformations parallels the strength of the intramolecular N−H···O hydrogen-bonding interactions. The N−H···O distances and angles suggest that the strength of these H-bonds follows the order AA_1 > AA_2 > BC_1 ≫ BC_2. In fact, a linear relationship is found to exist between the relevant geometric N−H···O parameters and the stability of the various conforma-

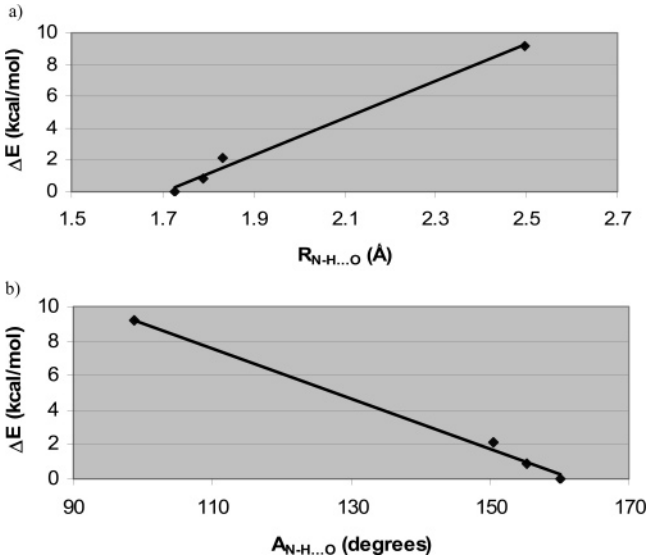

Figure 4. (a) MP2/6-31+G(d,p) relative energies of macrocycle conformations vs N−H···O=C H-bond distances. (b) MP2/6-31+G-(d,p) relative energies of macrocycle conformations vs N−H···O=C H-bond angles.

tions as shown in Figure 4. Additional evidence of the stabilizing role of the N−H···O hydrogen bonding is provided by the amount of electron density accumulated in the corresponding critical points as shown in Table 2. The presence of the N−H···O interactions is particularly important for AA_1 which, despite the lack of any inward C−H···O interactions, appears as the most stable conformation at the MP2 level. In sharp contrast, the lack of N−H···O interactions results in BC_2 being the least stable conformation despite its having both inward and outward C−H···O interactions.

To estimate whether macrocycle formation is likely to be exothermic or endothermic, we devise the following isodesmic reactions[21]

$$2A + 2(CH_3)CH{=}CH(CH_3) \rightarrow AA\_1 + 4CH_4 \qquad \Delta H_0 = -38 \text{ kcal/mol}$$

$$2A + 2(CH_3)CH{=}CH(CH_3) \rightarrow AA\_2 + 4CH_4 \qquad \Delta H_0 = -38 \text{ kcal/mol}$$

$$B + C + 2(CH_3)CH{=}CH(CH_3) \rightarrow BC\_1 + 4CH_4 \qquad \Delta H_0 = -40 \text{ kcal/mol}$$

$$B + C + 2(CH_3)CH{=}CH(CH_3) \rightarrow BC\_2 + 4CH_4 \qquad \Delta H_0 = -34 \text{ kcal/mol}$$

The reaction energies for the four reactions are calculated at the MP2/6-31+G(d,p) level and include the B3LYP/6-31+G-(d) ZPE corrections. In all cases, the reactions are estimated to be largely exothermic with the three more stable conformations having reactions energies close to one another as well as being more exothermic than the least stable conformation.

Harmonic Vibrational Frequencies of the Amide Motifs. The presence of intramolecular H-bonding interactions is manifested in several vibrational modes of the macrocycle, particularly the N−H and C=O stretching modes of the amide motifs which are displayed in Table 4 and Table 5, respectively. For example, the two stretching modes of the N−H units involved in H-bonding are significantly shifted to lower frequencies with respect to the outward N−H units not involved in H-bonding. The magnitude of the shift correlates well with the strength of the H-bond; using the more intense antisymmetric N−H mode, the strength of the N−H···O=C interaction follows the order AA_1 > AA_2 > BC_1 with corresponding red shifts of 247, 181, and 145 cm^{-1}. The lack of N−H···O=C interactions for BC_2 results in the inward N−H stretching modes being fairly close to those of the outward N−H modes. The vibrational results are in accord with the geometric and energetic results discussed previously. The inward N−H antisymmetric stretching modes have an acceptable correlation with the corresponding N−H bond distances as shown in the equation below

$$\nu_{N-H} = -19221R_{N-H} + 23049 \ (R^2 = 0.999)$$

TABLE 3: Relative Energies (kcal/mol) for B3LYP/6-31+G(d) Optimized Tetraamide Conformations and Diamide Motifs

6-31+G(d)				
system	ΔB3LYP	ΔHF	ΔMP2	ΔZPE
A	0.00	0.00	0.00	0.00
B	1.81	1.86	2.00	−0.10
C	2.78	3.04	2.55	−0.19
AA_1	0.00	0.00	0.00	0.00
AA_2	−1.14	0.26	0.93	−0.50
BC_1	1.23	1.38	2.16	−0.24
BC_2	9.54	7.15	9.51	−0.97

6-31+G(d,p)		
system	ΔHF	ΔMP2
A	0.00	0.00
B	1.87	1.94
C	3.07	2.47
AA_1	0.00	0.00
AA_2	0.17	0.86
BC_1	1.34	2.09
BC_2	7.27	9.17

6-311++G(2d,2p)		
system	ΔHF	ΔMP2
A	0.00	0.00
B	1.79	1.75
C	2.84	2.27

TABLE 4: B3LYP/6-31+G(d) N−H Stretching Frequencies (cm^{-1}) and Intensities (km/mol)

system	$(\nu_{N-H})^a$	$(\nu_{N-H})^b$	$(\nu_{N-H})^c$	$(\nu_{N-H})^d$	I_1	I_2	I_3	I_4
AA_1	3348	3353	3600	3600	0	1010	85	0
AA_2	3410	3413	3594	3594	66	652	42	18
BC_1	3448	3452	3597	3597	5	544	21	41
BC_2	3612	3612	3600	3600	13	4	17	30

[a] Inward N−H in phase; outward N−Hs do not move. [b] Inward N−H out of phase; outward N−Hs do not move. [c] Outward N−H out of phase; inward N−Hs do not move. [d] Outward N−H in phase; inward N−Hs do not move.

TABLE 5: B3LYP/6-31+G(d) C=O Stretching Frequencies (cm^{-1}) and Intensities (km/mol)

system	$(\nu_{C=O})^a$	$(\nu_{C=O})^b$	$(\nu_{C=O})^c$	$(\nu_{C=O})^d$	I_1	I_2	I_3	I_4
AA_1	1700	1700	1744	1745	472	0	417	0
AA_2	1703	1705	1741	1742	423	24	24	217
BC_1	1713	1718	1744	1745	13	326	250	275
BC_2	1744	1749	1756	1760	5	572	325	18

[a] Inward C=Os opposite phase. However, inward C=O in phase with the closer outward C=O. [b] All C=Os in phase. [c] Inward C=Os opposite phase. However, inward C=O in phase with the father outward C=O. [d] Inward C=Os in phase and opposite phase to outward C=Os.

TABLE 6: ^{1}H NMR (ppm) and Natural Atomic Charges (au) of the Inward N—H···O═C Interaction[a]

	H	O	^{1}H NMR
AA_1	0.482	−0.748	12.73
AA_2	0.479	−0.742	11.63
BC_1	0.474	−0.732	11.23
BC_2	0.432	−0.700	6.52

[a] ^{1}H NMR chemicals shifts are calculated at the B3LYP/6-311+G(2d,p) level and are presented relative to the standard TMS. NBO charges are calculated at the HF/6-31+G(d,p) level.

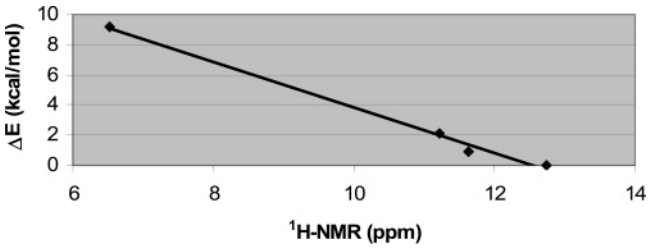

Figure 5. MP2/6-31+G(d,p) relative energies of macrocycle conformations vs the B3LYP/6-311+g(2d,p) ^{1}H NMR chemical shift of the amide hydrogen against the TMS standard.

The C═O stretching frequencies are displayed in Table 5. While the N—H stretching modes can be readily traced down to the strength of the N—H···O═C interactions, the C═O frequencies, on the other hand, are less suitable for such purpose because of their direct involvement in the additional weak C—H···O═C hydrogen-bonding interactions. However, the shift to lower frequencies of the inward C═O groups relative to the outward C═O groups suggests the order AA_1 > AA_2 > BC_1 for the strength of the N—H···O═C interactions, which is exactly the same order obtained using the N—H stretching modes. Because BC_2 lacks any N—H···O═C interactions, its inward C═O frequencies are much closer to the outward C═O frequencies.

Electron Density Shifts and ^{1}H NMR Chemical Shifts. Formation of the N—H···O═C hydrogen bond is expected to lessen the electron density on the bridging hydrogen and to augment that on the pertinent amide oxygen. Table 6 shows the natural population atomic charges for the amide hydrogen and oxygen atoms participating in the noted hydrogen bonding. BC_2 having no such interaction reveals the least positive charge for hydrogen and the least negative charge for the oxygen atom. The other three conformations undergo increases in the magnitude of the charges relative to BC_2, and the extent of these changes matches the strength of the H-bonds and the relative stability of the conformations.

Another key indicator of hydrogen-bond strength is the ^{1}H NMR chemical shift of the bridging amide hydrogen. The isotropic chemical shifts are reported in Table 6 relative to the standard TMS. Formation of the intramolecular N—H···O═C hydrogen bond produces a large shift to lower field. The extent of the shift correlates well with the strength of the interaction. Thus, the shift in AA_1 is 95% more than that of BC_2 which does not have this H-bond interaction; the corresponding shifts to lower fields for AA_2 and BC_1 are, respectively, 78% and 72% more than that of BC_2. The stabilizing role of the N—H···O═C hydrogen bond in the various conformations can be appreciated in Figure 5 which shows a reasonably linear correlation between the relative energies of the conformations and the chemical shifts of the inward amide hydrogen. Clearly, the stronger the N—H···O═C interaction, the more stable the macrocycle conformation. BC_2 lies highest in energy, which can be attributed to its lack of such an interaction.

TABLE 7: HF/6-31+G(d,p) NBO Second-order Stabilization Energies, $E^{(2)}$ (kcal/mol), Corresponding to the C═O···H—X (X = C, N) Interactions

		inward[a]	outward[a]
system	$n_O \rightarrow \sigma_{N-H}^*$	$n_O \rightarrow \sigma_{C-H}^*$	$n_O \rightarrow \sigma_{C-H}^*$
AA_1	28.49	0.00	1.44
AA_2	20.34	3.63	1.70
BC_1	18.23	2.52	1.46
BC_2	0.00	4.75	0.64

[a] A C═O···H interaction is labeled inward or outward based on whether such interaction points, respectively, toward or away from the central cavity upon formation of the macrocycle.

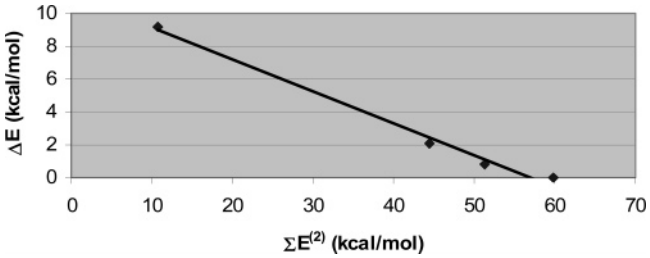

Figure 6. MP2/6-31+G(d,p) relative energies of macrocycle conformations vs the HF/6-31+g(d,p) NBO second-order stabilization energies of the amide oxygen lone pairs.

Perturbation Theory Energy Analysis. An examination of the possible interactions between "filled" (electron-donor) Lewis-type NBOs and "empty" (electron-acceptor) non-Lewis NBOs allows us to estimate their energetic importance by second-order perturbation theory. It is particularly appealing to investigate the Lewis−non-Lewis interactions stabilizing the lone pairs of an amide oxygen involved in either a C—H···O═C or N—H···O═C H-bonding interaction. The delocalization energies due to $n_O \rightarrow \sigma^*_{X-H}$ charge transfers (X = C or N) can be approximated by the formula[17]

$$E^{(2)}_{n\rightarrow\sigma^*} \approx (-2)F(n,\sigma^*)^2/(\epsilon_{\sigma^*} - \epsilon_n)$$

where ϵ_σ* and ϵ_n are diagonal elements (orbital energies) and $F(n,\sigma^*)$ is the corresponding off-diagonal NBO Fock matrix element. The results are displayed in Table 7. It is apparent that the inward C—H···O═C interaction provides a greater stabilization of the oxygen lone pairs than the outward interaction does. It is also evident that the N—H···O═C interaction is much stronger than either C—H···O═C interaction as indicated by the substantial stabilization of the pertinent oxygen lone pairs. The tabulated results can be used to demonstrate that the C—H···O═C interactions alone are insufficient to account for the relative stability of tetraamide conformations; no correlation is found between the relative energies of the conformations and $E^{(2)}$ if only weak C—H···O═C H-bonds are considered. However, addition of the delocalization energies of the oxygen lone pairs attributed to the much stronger N—H···O═C hydrogen bonds gives rise to an acceptable linear correlation as shown in Figure 6.

Aqueous Solution. The molecular dipole moments of the parent diamides and the macrocycle conformations are shown in Table 8. Also shown are the corresponding relative energies in a vacuum and in aqueous solvent using the 6-31+G(d) basis set and the MP2 and HF methods. As expected, differences in the molecular dipole moments result in important changes in the conformational preferences in aqueous solvent compared with the corresponding gas-phase (vacuum) results. The parent diamides fall within 1 kcal/mol from one another, with B now

TABLE 8: Dipole Moments (Debye) and Relative Energies (kcal/mol) of the Parent Motifs and Macrocycle Conformations in Water[a]

		HF		MP2	
system	μ	vacuum	water	vacuum	water
A	3.69	0.00	0.00	0.00	0.00
B	5.99	1.86	-0.79	2.00	-0.21
C	6.13	3.04	0.96	2.55	0.64
AA_1	0.00	0.00	0.00	0.00	0.00
AA_2	0.98	0.26	0.22	0.93	0.87
BC_1	9.92	1.38	-4.15	2.16	-4.59
BC_2	11.20	7.15	0.43	9.51	4.04

[a] The SCRF = dipole model and the 6-31+G(d) basis set were used for the calculations. Dipole moments were obtained using the B3LYP/6-31+G(d) level.

being the most stable diamide followed closely by A and then C. Because of their similar dipole moments, AA_1 and AA_2 have their relative energies only slightly changed in aqueous solution, with AA_1 still lying lower in energy. A more striking change is noted for the BC_1 and BC_2 conformations with the former being predicted to be the most stable conformer in water and the latter being energetically much closer to AA_1 and AA_2. In general, the qualitative changes going from vacuum to aqueous solvent are consistent in both HF and MP2 methods. The magnitude of the changes in the two methods also agrees within 1.3 kcal/mol. For example, BC_2 goes from a relative energy in a vacuum of 7.15 to 0.43 kcal/mol in water at the HF/6-31+G(d) level. Thus, BC_2 gains an additional stability of 6.72 kcal/mol thanks to its large dipole moment of 11.20 D. At the MP2 level, the gain is 5.47 kcal/mol which is about 1.3 kcal/mol less than the HF result. It is worth noting that, while the HF method brings BC_2 quite close in energy to AA_1 and AA_2, the MP2 method still places BC_2 at a much higher energy. Because of the inherent limitations of the Onsager model, the results presented here are to be interpreted as modest approximations to solvent effects. In particular, calculations performed on systems such as AA_1, with no net dipole moment, will give the same results as those for the gas phase.

Summary and Outlook

We have presented an ab initio study of the structure of a model macrocycle tetraamide. The four amide groups in the selected model are present in the sequence: −(O═CNH)−Ph−(NHC═O)−CH═CH−(O═CNH)−Ph−(NHC═O)−CH═CH−. Here, two phenyl rings and two ethenyl groups bridge the amide units. Each amide motif bonds to a phenyl ring through its amide nitrogen and to an ethenyl group through its amide carbon. Four minimum-energy conformations conveniently labeled AA_1, AA_2, BC_1, and BC_2 were identified (Figures 2 and 3). Suitable isodesmic reactions suggest that the formation of the macrocycle tetraamide in any of the above conformations is thermodynamically favorable by more than 30 kcal/mol. Also, the methods employed suggest the following conformational preference in the gas phase AA_1 > AA_2 > BC_1 ≫ BC_2. Intramolecular hydrogen-bonding interactions of the type N−H···O═C and C−H···O═C appear as the major stabilizing factors of the different conformations. The strength of these interactions matches the calculated stability order. Several key indicators such as N−H and C═O bond lengths and vibrational stretching modes, ^{1}H NMR chemical shifts, and electron density at the H-bond critical points were employed to assess H-bond strength. Natural bond orbital analysis was performed to estimate the delocalization interactions stabilizing the lone pairs of an amide oxygen involved in either a C−H···O═C or N−H···O═C H-bonding interaction. It is found that the combined delocalization energies resulting from $n_O \rightarrow \sigma^*_{X-H}$ charge transfers (X = C or N) have an acceptable linear correlation with the stability of the various conformations. The relative strength of N−H···O vs C^α−H···O hydrogen bonds in amides has been previously studied by Vargas et al.[22] The results of such a study show that, when coupled with the N−H···O hydrogen bond in a β-sheet, the C^α−H···O hydrogen bond would enhance the interaction by 60%. It was suggested then that C^α−H···O hydrogen bonds contribute significantly to the overall stabilization secondary and tertiary protein structure. The suggested important stabilizing role of C−H···O hydrogen bonds appears supported in the present study. In aqueous phase, the conformational preference changes to BC_1 > AA_1 > AA_2 > BC_2, which can be attributed mainly to differences in molecular dipole moments.

Our interest in macrocycle amides is driven primarily by their potential ability to bind cations and anions thanks to the amphiphilic properties of the amide group. Current efforts are directed to investigate the alkali and alkaline earth metal ions binding affinity as well as anion (F^-, Cl^-) affinity of the model macrocycle amide studied in this work; the results of such work will be published elsewhere. Of particular interest is the induced conformational change upon ion binding which should result in well-defined cavities with convergent arrangement of the amide carbonyl groups or hydrogens to bind the cations or anions, respectively.

Acknowledgment. We are particularly grateful for the financial support provided by the Chemistry Department at DePaul University.

Supporting Information Available: Cartesian coordinates for the B3LYP/6-31+G(d) optimized structures for the three parent motifs and the four conformations of the macrocycle are presented. Also provided are tables with the absolute energies at the various levels of theory of all the structures in this work in the gas phase and in aqueous solution. This material is available free of charge via the Internet at http://pubs.acs.org.

References and Notes

(1) (a) Lehn, J.-M. *Supramolecular Chemistry*; VCH: Weinheim, Germany, 1995. (b) Schneider, H.-J.; Yatsimirsky, A. *Principles and Methods in Supramolecular Chemistry*; Wiley: Chichester, U.K., 2000. (c) Steed, J. W.; Atwood, H. L. *Supramolecular Chemistry*; Wiley: Chichester, U.K., 2000. (d) Dietrich, B.; Viout, P.; Lehn, J.-M. *Macrocyclic Chemistry*; VCH: Weinheim, Germany, 1993.

(2) Dearden, D. V.; Liang, Y.; Nicoll, J. B.; Kellesberger, K. A. *J. Mass Spectrom.* **2001**, 36, 989. (b) Schneider, H. J. *Angew. Chem., Int. Ed. Engl.* **1991**, *30*, 1417.

(3) (a) Pedersen, C. J. *J. Am. Chem. Soc.* **1967**, *89*, 2495. (b) Pedersen, C. J. *Angew. Chem., Int. Ed. Engl.* **1988**, *27*, 1021. (c) Glendening, E. D.; Feller, D. Thompson, M. A. *J. Am. Chem. Soc.* **1994**, *116*, 10657. (c) Glendening, E. D.; Feller, D. *J. Am. Chem. Soc.* **1996**, *118*, 6052.

(4) Lehn, J.-M. *Acc. Chem. Res.* **1978**, *11*, 49.

(5) Cui, C.; Cho, S. J.; Kim, S. *J. Phys. Chem. A* **1998**, *102*, 1119.

(6) Lee, W. Y.; Park, C. H.; Kim, S. *J. Am. Chem. Soc.* **1993**, *115*, 1184.

(7) Szejtli, J.; Osa, T. *Comprehensive Supramolecular Chemistry*; Cyclodextrines; Atwood, J. L., Davies, J. E. D., MacNicol D. D., Vögtle, F., Eds.; Elsevier: Oxford, U.K., 1996; Vol. 3.

(8) (a) Casnati, A.; Baldini, L.; Pelizzi, N.; Rissanen, K.; Ugozzoli, F.; Ungaro, R. *J. Chem. Soc., Dalton Trans.* **2000**, 3411. (b) Perrin, M.; Oehler. In *Calixarenes, a Versatile Class of Macrocyclic Compounds*; Vicens, J., Böhmer, V., Eds.; Kluwer Academic Publishers: Dordrecht, The Netherlands, 1991.

(9) (a) Kim, H. Y.; Calabrese, J.; McEwen, C. *J. Am. Chem. Soc.* **1996**, *118*, 1545. (b) Kim, K. S.; Cui, C.; Cho, S. *J. Phys. Chem. B* **1998**, *102*,

461. (c) Malinowska, E.; Wróblewski, W.; Ostaszewski, R.; Jurczak, J. *Pol. J. Chem.* **2000**, *74*, 701. (c) Chmielewski, M.; Jurczak, J. *Tetrahedron Lett.* **2004**, *45*, 6007. (d) Szczepañska, A.; Sa×b8añski, P.; Jurczak, J. *Tetrahedron* **2003**, 4775. (e) Hossain, Md. A.; Llinares, J. M.; Powell, D.; Bowman-James, K. *Inorg. Chem.* **2001**, *40*, 2936. (f) Hossain, Md. A.; Kang, S. O.; Powell, D.; Bowman-James, K. *Inorg. Chem.* **2003**, *42*, 1397. (g) Suh, S. B.; Cui, C.; Son, H. S.; U., J. S.; Won, Y.; Kim, K. S. *J. Phys. Chem. B* **2002**, *106*, 2061. (h) Chmielewski, M.; Szumna, A.; Jurczak, J. *Tetrahedron Lett.* **2004**, *45*, 8699. (i) Filippi, A.; Gasparrini, F.; Pierini, M.; Speranza, M.; Villani, C. *J. Am. Chem. Soc.* **2005**, *127*, 11912. (j) Chmielewski, M.; Jurczak, J. *Chem.*−*Eur. J.* **2005**, *11*, 6080.

(10) Frisch, M. J.; Trucks, G. W.; Schlegel, H. B.; Scuseria, G. E.; Robb, M. A.; Cheeseman, J. R.; Montgomery, J. A., Jr.; Vreven, T.; Kudin, K. N.; Burant, J. C.; Millam, J. M.; Iyengar, S. S.; Tomasi, J.; Barone, V.; Mennucci, B.; Cossi, M.; Scalmani, G.; Rega, N.; Petersson, G. A.; Nakatsuji, H.; Hada, M.; Ehara, M.; Toyota, K.; Fukuda, R.; Hasegawa, J.; Ishida, M.; Nakajima, T.; Honda, Y.; Kitao, O.; Nakai, H.; Klene, M.; Li, X.; Knox, J. E.; Hratchian, H. P.; Cross, J. B.; Bakken, V.; Adamo, C.; Jaramillo, J.; Gomperts, R.; Stratmann, R. E.; Yazyev, O.; Austin, A. J.; Cammi, R.; Pomelli, C.; Ochterski, J. W.; Ayala, P. Y.; Morokuma, K.; Voth, G. A.; Salvador, P.; Dannenberg, J. J.; Zakrzewski, V. G.; Dapprich, S.; Daniels, A. D.; Strain, M. C.; Farkas, O.; Malick, D. K.; Rabuck, A. D.; Raghavachari, K.; Foresman, J. B.; Ortiz, J. V.; Cui, Q.; Baboul, A. G.; Clifford, S.; Cioslowski, J.; Stefanov, B. B.; Liu, G.; Liashenko, A.; Piskorz, P.; Komaromi, I.; Martin, R. L.; Fox, D. J.; Keith, T.; Al-Laham, M. A.; Peng, C. Y.; Nanayakkara, A.; Challacombe, M.; Gill, P. M. W.; Johnson, B.; Chen, W.; Wong, M. W.; Gonzalez, C.; Pople, J. A. *Gaussian 03*, revision C.02.; Gaussian, Inc.: Wallingford, CT, 2004.

(11) Stephens, P. J.; Devlin, F. J.; Chabalowski, C. F.; Frisch, M. J. *J. Phys. Chem.* **1994**, *98*, 11623.

(12) Becke, A. D. *J. Chem. Phys.* **1993**, *98*, 5648.

(13) Hariharan, P. C.; Pople, J. A. *Theor. Chim. Acta* **1973**, *28*, 213.

(14) Clark, T.; Chandrasekhar, J.; Spitznagel, G. W.; Schleyer, P. v. R. *J. Comput. Chem.* **1983**, *4*, 294.

(15) Francl, M. M.; Pietro, W. J.; Hehre, W. J.; Binkley, J. S.; Gordon, M. S.; DeFrees, D. J.; Pople, J. A. *J. Chem. Phys.* **1982**, *77*, 3654.

(16) Møller, C.; Plesset, M. S. *Phys. Rev.* **1934**, *46*, 618.

(17) (a) Foster, J. P.; Curtiss, L. A.; Weinhold, F. *J. Am. Chem. Soc.* **1980**, *102*, 7211. (b) Reed, A. E.; Curtiss, L. A.; Weinhold, F. *Chem. Rev.* **1988**, *88*, 899. (c) Glendening, E. D.; Reed, A. E.; Carpenter, J. E.; Weinhold, F. *Nbo*, version 3.1.

(18) (a) Bader, R. F. W. *Atoms in Molecules. A Quantum Theory*; Oxford University Press: New York, 1990. (b) Cioslowski, J.; Nanayakkara, A.; Challacombe, M. *Chem. Phys. Lett.* **1993**, *203*, 137. (c) Cioslowski, J.; Surjan, P. R. *J. Mol. Struct. (THEOCHEM)* **1992**, *255*, 9.

(19) Wolinski, K.; Hilton, J. F.; Pulay, P. *J. Am. Chem. Soc.* **1990**, *112*, 8251.

(20) (a) Onsager, L. *J. Am. Chem. Soc.* **1938**, *58*, 1486. (b) Kirkwood, J. G. *J. Chem. Phys.* **1934**, *2*, 351.

(21) Wiberg, K. B.; Hadad, C. M.; Rablen, P. A.; Cioslowski, J. *J. Am. Chem. Soc.* **1992**, *114*, 8644.

(22) Vargas, R.; Garza, J.; Dixon, D. A.; Hay, B. P. *J. Am. Chem. Soc.* **2000**, *122*, 4750.